

Shots and variance on noisy quantum circuits

MANAV SEKSARIA^{1,2}, ANIL PRABHAKAR^{1,2}

¹Centre for Quantum Information, Communication and Computing, Indian Institute of Technology Madras, Chennai, India

²Department of Electrical Engineering, Indian Institute of Technology Madras, Chennai, India

ABSTRACT We present a method for estimating the number of shots required for some desired variance in the results of a quantum circuit. First, we establish a baseline for a single qubit characterization of individual noise sources separately. We then extend the method to multi-qubit problems and test our method on two case studies. We will proceed to estimate the number of shots required for a desired variance in the result or, equivalently estimate the variance at a known number of shots. We will show we're able to estimate variance accurately to within a factor of 2. Following these, we also provide a closed-form expression for variance at a given number of shots.

INDEX TERMS Quantum Computing, Quantum Circuits, Statistical Analysis

I. INTRODUCTION

Quantum computers are expected to provide exponential speed-ups in solving certain problems [1], [2]. However, the current era of quantum computing, often referred to as the Noisy Intermediate-Scale Quantum (NISQ) era, is characterized by devices with a limited number of qubits that are prone to errors and decoherence [3]. Naturally, since the machines are noisy we run each circuit multiple times to get a reliable result. The number of times we run the circuit is called the number of shots. The ideal number of shots is a tradeoff between the precision of the result and the computational cost of running each shot.

In this work, we explore the problem of estimating the number of shots required to achieve the desired precision in the results, where precision is quantified by the variance. There has been significant work done discussing the convergence of VQEs with unbiased estimators on various algorithms [4], [5]. These convergence studies however apply only to noiseless systems and need to be extended to noisy systems for each run. At the same time, there has been work done on the distribution of noise in individual qubits [6], [7]. Recently there have been more empirical methods used, where the number of shots is determined by running the circuit multiple times and adjusting the number of shots until a satisfactory result is achieved through trial and error [8], [9], Barron et al. [10] have also found better bounds for the overhead in variance due to noise for specific algorithms.

In this work, we work in regimes where error correction

is not applied, since decoherence time is then effectively infinity [11], making finding variance much harder. We aim to provide a systematic framework for estimating the number of shots required to achieve a desired variance in our results, for NISQ-era machines. We develop a statistical analysis of various noise sources and their impact on shot estimation. We rely on the Central Limit Theorem (CLT) as a tool to convert the obtained distributions into a malleable form. We first apply CLT to individual qubits' noise sources and see how it affects the variance of the results. These methods are then generalized to apply to larger circuits with multiple-qubit circuits. Since the general class of all multi-qubit quantum circuits would be intractable, we look at the sub-class of circuits with expectation value type problems for Hermitian observables.

We work with four basic sources of noise that we assume are independent of each other. Therefore, if we treat them as four random variables X_i , then $\text{Covar}(X_i, X_j) = 0, \forall i \neq j$. Additionally, since we assume independent sources of noise it also implies that our sources of noise are assumed to be independent of the circuit run. We deal primarily with four forms of well-studied noise sources: SPAM noise, amplitude damping (T_1), phase damping (T_2), and gate noise [12], [13]. We then combine these sources of noise to get a general formula for shot estimation which is then tested on two case studies. For both case studies, we compare the predicted shot counts with experimental data.

While we focus on superconducting qubits, these methods

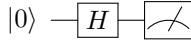


FIGURE 1: Circuit baseline fair coin toss.

may be generalized to other realizations of qubits, since they contain similar types of errors at different magnitudes [14], [15]. There are also significant sources of errors in the form of correlated errors and crosstalk that are excluded from the analysis due to the lack of widely accepted models [16], [17].

II. SINGLE QUBIT EXPERIMENTS

We start with a single qubit experiment of a Hadamard gate as the baseline and evaluate this circuit (Fig. 1) on a simulator and a QPU to obtain a coin toss distribution. For a noiseless simulator, we expect a perfectly balanced distribution of 0, 1 for the qubit. We find the expectation of the measurement Z taken n times as $\mu = E[X] = \sum_{i=1}^n x_i p_i$ such that p_i is the probability of x_i , for all events x_i in the sample space. We expect $\mu \rightarrow \mu_0$ as $n \rightarrow \infty$ with $\mu_0 = 0.5$ for a fair coin toss.

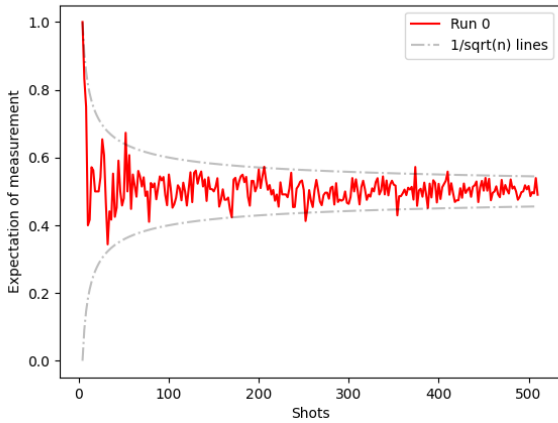


FIGURE 2: As more shots are taken the width of the distribution falls off as $1/\sqrt{n}$.

Fig. 2 confirms our expectation of $\mu \rightarrow 0.5$ as n increases. We also observe the width of the distribution falls off as $1/\sqrt{n}$ (overlaid for clarity). We will now use this plot as a baseline for all individual sources of noise and see how they affect the distribution.

III. INDIVIDUAL NOISE SOURCES

State Preparation And Measurement (SPAM) errors arise either during the preparation of the qubit or during measurement. IBM's current noise simulators only allow us to simulate readout errors. For now, we **assume** are negligible. Readout errors are made up of components: $p_{0 \rightarrow 1}$ and $p_{1 \rightarrow 0}$, the probability of a '0' being read as a '1' and the reverse respectively. We write the modified expectation as,

$$\mu' = P(1) + p_{0 \rightarrow 1}P(0) - p_{1 \rightarrow 0}P(1). \quad (1)$$

This implies, that when plotted with asymmetric readout error ($p_{0 \rightarrow 1} \neq p_{1 \rightarrow 0}$) we should see a shift in net expectation value. We have plotted the results for three cases:

- Symmetric readout errors on IBM Qiskit noisy simulator: (0, 0)
- Symmetric readout errors on an independent noisy simulator presented in [18]: (0.33, 0.33)
- Asymmetric readout errors on IBM Qiskit noisy simulator: (0.33, 0.5)

We see, that the expectation for symmetric readout errors is the same as a fair coin, whereas in the asymmetric case, the expectation is shifted (see Fig. 3), confirming our calculations.

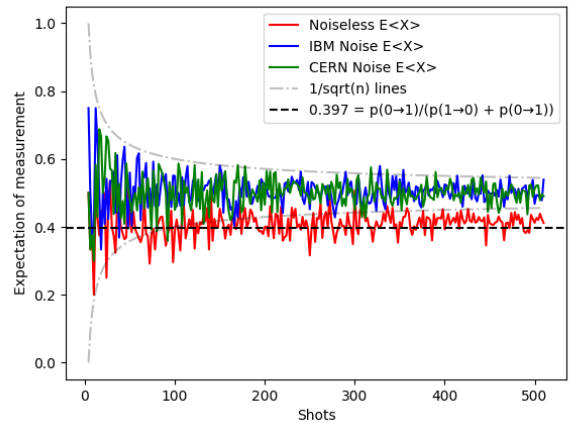


FIGURE 3: When we add asymmetric noise to the coin toss the distribution shifts, down. Whereas, for symmetric noise, the mean is independent of the amount of noise.

A. CENTRAL LIMIT THEOREM AND RELATIVE STANDARD DEVIATION

Having seen the standard deviation consistently fall off as $1/\sqrt{n}$, we can now use a slightly modified metric of σ/μ , or the relative standard deviation (RSD) to measure the spread of the distribution. R3SD has the advantage of being dimensionless and therefore can be used to compare distributions across different scales. We can then plot $\log(\text{RSD})$ vs $\log(w)$ where w is a window size, defined as follows:

We first convert our distribution X to a new distribution \bar{X}_w by taking mean of windows of w shots, such that $\bar{X}_w = \{\mu_{w,1}, \mu_{w,2}, \dots, \mu_{w,n/w}\}$ as mean of subsets of values $[x_i, x_{i+w}] \in X$. From the classical central limit theorem, we know, that \bar{X}_w will be normally distributed as $w \rightarrow \infty$. We can then plot $\log(\text{RSD})$ vs $\log(w)$ for various values of w . The algorithm is listed in Algorithm 1.

Algorithm 1 Conversion to Normal Distribution.

```

1:  $N \leftarrow 256$  {Number of windows}
2:  $S \leftarrow 2^{15}$  {Total shots}
3:  $W \leftarrow \{2^2, 2^3, 2^4, 2^5, 2^6, 2^7\}$  {Window sizes}
4: for each  $w \in W$  do
5:   Divide results into  $N$  windows of size  $w$ 
6:   for each window  $i$  do
7:     Compute mean  $\mu_i$  for each window  $i = 1, 2, \dots, N$ 
8:   end for
9:   Compute mean  $\mu$  and standard deviation  $\sigma$  of  $\{\mu_i\}$ 
10:  Store  $\log(\frac{\sigma}{\mu})$  and  $\log(w)$ 
11: end for
    
```

B. SPAM NOISE

1) Simulation

Running the SPAM experiments again, for the three cases, with no noise and with symmetric noise ($p_{0 \rightarrow 1} = p_{1 \rightarrow 0} = 0.33$) but on different simulators, we can see the results of the experiments in Fig. 4:

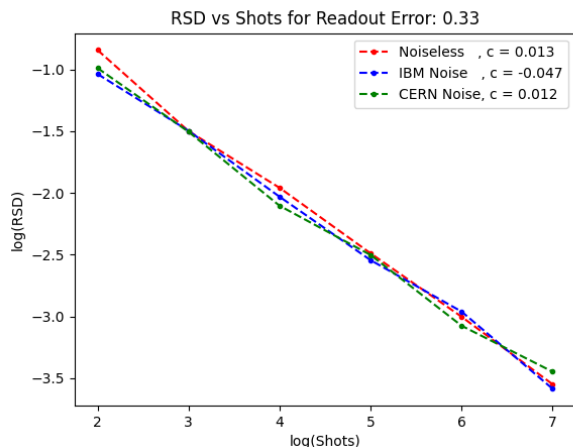


FIGURE 4: Variance falls off as $1/\sqrt{n}$, therefore naturally in log scale we expect a slope of $-1/2$.

Treating the distribution as CLT, we now know we expect $c = y - mx$ where $m = -1/2$ and $c = \log(\sigma/\mu)$. We calculate the expected c values for each of the three cases and compare them to the actual values. For a binomial distribution, we derive c as:

$$\begin{aligned}
 c &= y - mx \\
 &= \log(\sigma/\mu) + \frac{1}{2} \log(w) \\
 &= \log(\sqrt{wp(1-p)/wp}) + \frac{1}{2} \log(w) \\
 &= \frac{1}{2} \log\left(\frac{1-p}{p}\right) = \frac{1}{2} \log\left(\frac{p_0}{p_1}\right) \quad (2)
 \end{aligned}$$

Since $p \in (0, 1) \implies c \in (-\infty, 0)$, and as $p_1 = p$ increases, the line shifts down.

2) Hardware

From (Eq. c:coin) we expect

$$\Delta c = c_2 - c_1 = \frac{1}{2} \log\left(\frac{1-p_1}{p_1} \frac{p_2}{1-p_2}\right), \quad (3)$$

for some two different coin toss distributions with parameters p_1, p_2 . We can treat $p_1 = 0.5$ as a fair coin, and p_2 as a biased coin, such that the probabilities of readout error have been accounted for in p_2 itself as done in (1). p_1, p_2 now represent a fair coin and a SPAM noisy coin respectively, letting us then write c for SPAM noise as

$$c_{\text{pred}} = \frac{1}{2} \log\left(\frac{1+p_{0 \rightarrow 1} - p_{1 \rightarrow 0}}{1+p_{1 \rightarrow 0} - p_{0 \rightarrow 1}}\right). \quad (4)$$

This implies all symmetric SPAM noise models should have $c = 0$ since $p_{0 \rightarrow 1} = p_{1 \rightarrow 0}$. Additionally, if this values of $p_{0 \rightarrow 1}, p_{1 \rightarrow 0} \rightarrow 0$ we should have $c \rightarrow 0$. We can also see that, if one of the readout errors is 0 and the other is some $x \in (0, 1)$, c is highly sensitive to x as $\frac{dc}{dx} = \pm 2/(x^2 - 1)$. This would imply, that as we get closer to a higher probability of a ‘uni-directional’ readout error, our variance explodes. We would therefore prefer both small and symmetric readout errors.

We test our result for c_{pred} on the IBM Torino machine and see if we can predict the c values for the qubits. From Table 1 we can see that we can predict the c values within 0.01 of the actual value from just the calibration data. We can see also that the c values are generally also more negative since we expect more noise than we account for with only SPAM. It is unknown why Qubit 61 has a higher error in our prediction for c value than the other qubits. We hypothesize that Qubit 61 has either other sources of noise acting or the calibration data was outdated due to two days of queue time to account for our error.

TABLE 1: Qubit parameters from IBM Torino’s calibration and comparable values of c .

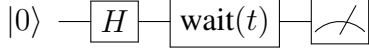
Qubit	T_1	$p_{0 \rightarrow 1}$	$p_{1 \rightarrow 0}$	Expected c	Actual c
61	232	0.0099	0.006	-0.01	-0.13
129	232	0.0186	0.014	-0.012	-0.012
5	232	0.0350	0.0428	0.023	0.033

C. T_1 NOISE

T_1 decay increases the probability of a qubit going from $|1\rangle$ to $|0\rangle$ over time. We can test for T_1 by modifying our circuit to wait for some known time before measurement and then adding a decay to our coin toss experiment. We will apply ‘wait’ in time multiples of δt (time unit for pulse operations which IBM refers to as dt) for single qubits gates for the IBM Torino system. Our ‘wait’ gate will be implemented not only as identity (Id) but also X, H gates to account for single qubit gate noise. Therefore $\text{wait}(n) = \text{Id}^n, X^n, H^n$ gates. Let us define $\epsilon = e^{-t/T_1}$ [13] and write modified expressions

$$p'_0 = p_0 + p_1 \epsilon, \quad (5)$$

$$p'_1 = p_1 - p_1 \epsilon. \quad (6)$$


 FIGURE 5: Circuit for T_1 noise with variable wait.

and substitute them back into the SPAM formula giving us,

$$c_{\text{pred}} = \frac{1}{2} \log \left(\frac{b(1 - p_{0 \rightarrow 1}) + p_{1 \rightarrow 0}}{b(p_{0 \rightarrow 1}) + 1 - p_{1 \rightarrow 0}} \right), \text{ where } b = \frac{1 + \epsilon}{1 - \epsilon}. \quad (7)$$

We observe that when $\epsilon \rightarrow 0 \implies b \rightarrow 1$ and we regress to the SPAM noise formula.

We compare c_{pred} to c_{real} as $\Delta_{\epsilon} c = |c_{\text{pred}} - c_{\text{real}}|$ after running the modified coin toss circuit in Fig. 5 on IBM Torino's hardware. We have mapped the results (from appendix Table 8) onto the qubit architecture image for ease of visualization. We can then see the results for T_1 noise in Fig. 6 and Fig. 7. The color scheme for the results is defined in Table 2 and Table 3. We can draw the obvious conclusion that

TABLE 2: Color Scheme for Results.

$\Delta_{\epsilon} c$	σ Ratio	Color	Meaning
< 0.5	< 1.41	green	Correct Prediction
$0.5 - 1.0$	$1.41 - 2$	yellow	Approximate, Other noise
> 1.0	> 2	black	Bad Qubit/Wrong Model

 TABLE 3: Color Scheme for T_1, T_2 on Torino system map.

T_1 Range	Color
$-\infty - -1.5\sigma$	red
$-1.5\sigma - 0\sigma$	orange
$0\sigma - 1.5\sigma$	yellow
$1.5\sigma - \infty$	green

we are able to predict short-depth circuits (10 gates) more accurately than long-depth (1000 gates). We also see that bad 'connections' and/or low T_1 qubits show up reliably as errors and may affect even single shared neighbor qubits. It is also easy to conclude that predictions are more accurate for Id gates than X, H gates. H gates have disproportionately high errors, which could be due to higher specific gate errors that do not show up in randomized benchmarking [19]. We follow a similar procedure for T_2 noise and see if we can predict the c values for the qubits.

D. T_2 NOISE

T_2 decay makes the probability of a qubit going from any known phase, say $|+\rangle$, to a uniform superposition of $|+\rangle$ and $|-\rangle$ increase over time. Equivalently, the probability of a Z gate being applied to a qubit increases as $p \propto 1 - e^{-t/T_2}$. As before let us define $\epsilon_1 = e^{-t/T_1}$, $\epsilon_2 = e^{-t/T_2}$. If we then apply a T_1, T_2 noisy channel onto a density matrix we get the resultant state as [13]

$$\rho_{T_1+T_2} = \begin{pmatrix} 1 + (|a|^2 - 1)\epsilon_1 & ab^*\epsilon_2 \\ a^*b\epsilon_2 & |b|^2\epsilon_1 \end{pmatrix}. \quad (8)$$

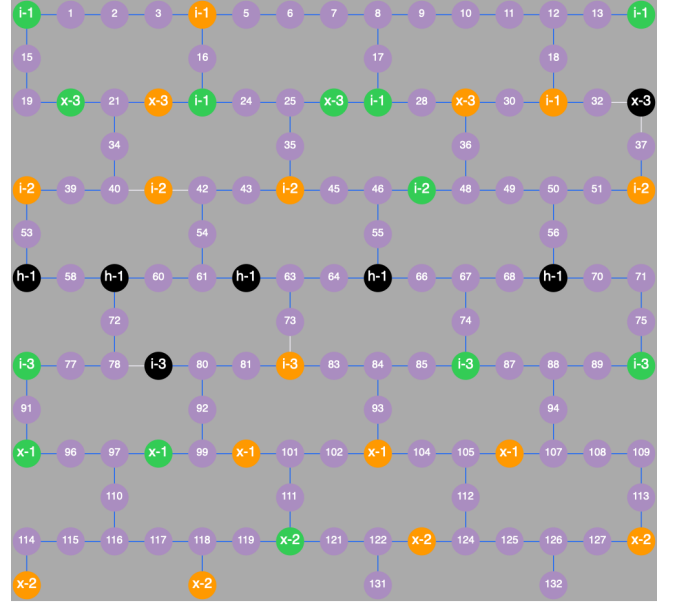


FIGURE 6: T1 results.

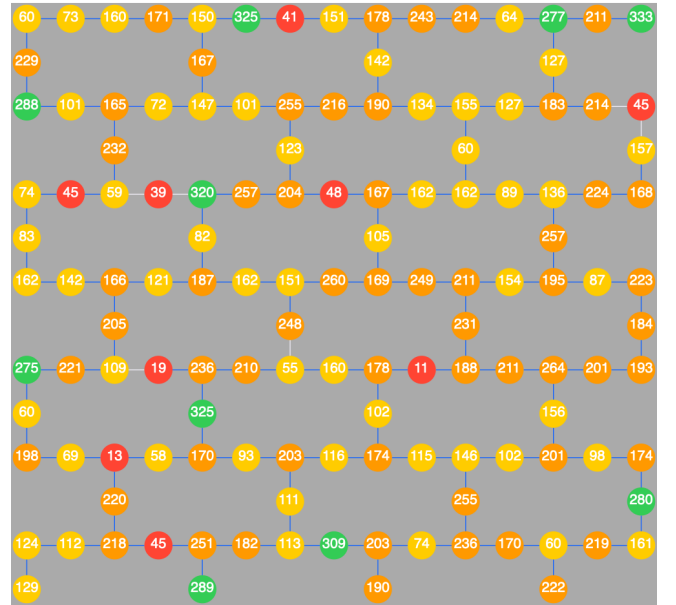


FIGURE 7: Torino T1 Map.

Multiplying by the H gate matrix, we get probabilities for the coin-toss experiment with T_2 in H basis.

$$c = \frac{1}{2} \log \left(\frac{b(1 - p_{0 \rightarrow 1}) + p_{1 \rightarrow 0}}{b(p_{0 \rightarrow 1}) + 1 - p_{1 \rightarrow 0}} \right), \text{ where } b = \frac{1 + \epsilon_2}{1 - \epsilon_2}. \quad (9)$$

As before, $\text{wait}(n) = \text{Id}^n, X^n, H^n$ gates. Additionally, since we run a grid of experiments at once, we ran the left half with extra measurements before the circuit (Fig. 9) and

$$|0\rangle \text{ --- } [H] \text{ --- } [\text{wait}] \text{ --- } [H] \text{ --- } [\text{meter}] \quad (10)$$

 FIGURE 8: Circuit for T_2 noise.

$$|0\rangle \text{ --- } [\text{meter}] \text{ --- } [H] \text{ --- } [\text{wait}] \text{ --- } [H] \text{ --- } [\text{meter}] \quad (11)$$

 FIGURE 9: Circuit T_2 with pre-measurements.

the right half (Fig. 8) without, to see if pre-measurement can reduce any form of error. Our circuits to execute now modify from the one run for T_1 noise to ones shown in Fig. 8 and Fig. 9.

We have color-coded the T_2 results with the same color scheme and mapped it onto the system architecture to visualize the values (see appendix Table 9), as is visible in Fig. 10 and Fig. 11. The black line is the dividing line between the two halves of the circuit, we applied pre-measurements to all the experiments on the LEFT half and ran the RIGHT half without pre-measurements.

We can see that the mean $\Delta_\epsilon c$ is higher than T_1 i.e. we are worse at predicting T_2 than T_1 . We can also see that the results for X gate seem to be more reliable than Id gates. Considering that X will add gate noise, we suspect this is because we are underestimating T_2 noise via the normal model of e^{-t/T_2} . There may either be a slight stretching in the exponent (as some $(-t/T_2)^k$), or a correction being applied in the backend that we have not accounted for.

By virtue of being constructed from the Central Limit Theorem, one may even generate confidence levels for their obtained intervals with little effort. Additionally, while here we have chosen to neglect it due to very small values, one may choose to go for an even broader range of acceptable $\Delta_\epsilon c$ by accounting for uncertainty in T_1, T_2 itself as follows. Let's say the uncertainty in T_2 is some σ_{T_2} , then the uncertainty in c is given by,

$$\sigma_c = \frac{\partial c}{\partial T_2} \sigma_{T_2}. \quad (12)$$

We have defined c for the T_2 experiment as (9). Let us say we were to ignore the readout error for now and account only for T_2 , we can write $\sigma_c = \frac{\partial c}{\partial T_2} \sigma_{T_2}$ as,

$$\sigma_c = \frac{te^{t/T_2}}{T^2(e^{2t/T_2} - 1)} \sigma_{T_2}. \quad (13)$$

Therefore if we have $T_2 = 500\delta t$ at some circuit depth $t = 100\delta t$, then for $\sigma_{T_2} = 20\delta t$ we will have $\sigma_c = 0.02$. We can see that as T_2 increases, the uncertainty in c falls as $1/T_2^2$, therefore for large enough T_2 values, the uncertainty in c will be very small. We can also see $t \rightarrow 0$ would imply $\sigma_c \rightarrow 0$.

IV. GENERALISATION

Having established our method works, and covered the major sources of noise, we will now generalize. Let our observable

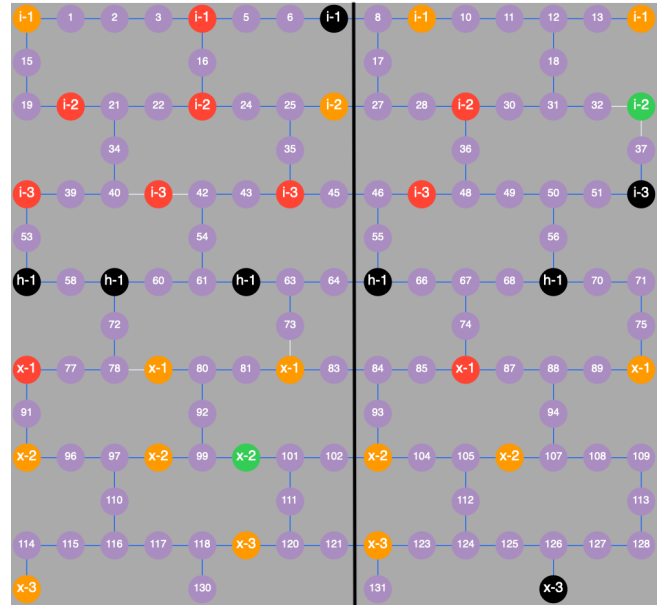


FIGURE 10: T2 results.

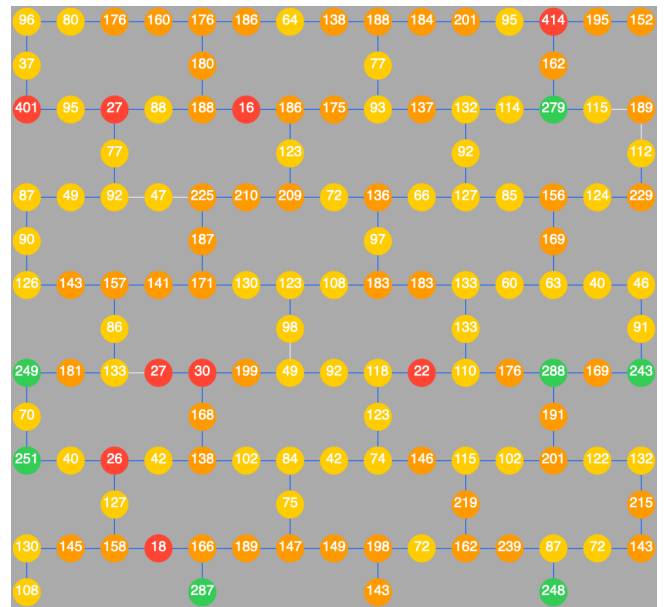


FIGURE 11: Torino T2 Map.

be some Hermitian H , with some X_i sources of noise. We can then write the variance of the noisy observable as

$$\text{Var}(H_\epsilon) = \text{Var}(H) + \sum_i \text{Var}(X_i), \quad (14)$$

such that we have assumed all sources of noise are independent i.e. $\text{covar}(X_i, X_j) = 0$. Now we may reasonably assume that for some fixed state ψ , the noise around our state is, as an aggregate, normally distributed. We write the variance of

our observable as

$$c = \log(\sqrt{\sigma^2/\mu^2}) = \frac{1}{2} \log\left(\frac{\text{Var}(H_\epsilon)}{\langle H \rangle^2}\right) \\ = \frac{1}{2} \log\left(\frac{\Delta H + \sum_i (E[X_i^2] - E[X_i]^2)}{\langle H \rangle^2}\right). \quad (15)$$

Since we are now working in log scale, we can afford to have approximate values everywhere, as a result of which we will take only first-order approximations of all forms of noise. Additionally as long as $\langle H \rangle \gg 0$, the value of c will be relatively insensitive to the value of $\langle H \rangle$. For some constant standard deviation $\sigma_{\langle H \rangle}$,

$$\sigma_c = \frac{\partial c}{\partial \langle H \rangle} \sigma_{\langle H \rangle} \\ = \frac{\partial}{\partial \langle H \rangle} \log\left(\frac{\sigma_{\langle H \rangle}}{\langle H \rangle}\right) \sigma_{\langle H \rangle} \\ = -\frac{\sigma_{\langle H \rangle}}{\langle H \rangle}. \quad (16)$$

To estimate the variance of our observable, one may choose to use approximate sampling methods or random states to estimate the variance of the observable or we can follow a two-step process where we first select an upper bound on the variance of the observable and then correct it.

A. METHODS OF EXTRACTING VARIANCE

1) Sampling Methods

For approximatable systems, we can use sampling methods to estimate the variance of the observable, via

$$\text{Var}(H_{\psi_i}) = \langle \psi | H^2 | \psi \rangle - \langle \psi | H | \psi \rangle^2 \quad (17)$$

on some states $\{|\psi_i\rangle\}$, and take

$$\text{Var}(H) = \frac{1}{n} \sum \text{Var}(H_{\psi_i}) \quad (18)$$

where n is the number of states sampled. The states sampled chosen here may be chosen to be specific to the problem, or from a Haar random distribution of states depending on the problem.

2) Known Range

For observables, such as molecule Hamiltonians [2], where we may know approximate values of max, min, and expected value of the distribution we can use Popoviciu's inequality on variances as

$$\sigma^2 \leq \frac{1}{4} (\lambda_{\max} - \lambda_{\min})^2, \quad (19)$$

such that λ_i are the eigenvalues of the observable. Or to obtain a tighter bound on the variance

$$\sigma^2 \leq (\max - \langle H \rangle)(\langle H \rangle - \min), \quad (20)$$

depending on which values are approximately known (via Bhatia-Davis inequality) [20].

3) Sum of Coefficients

If however none of the above values are known, we can use the sum of coefficients of the observable's terms expressed as a function of Pauli operators as a very loose upper bound on the variance of the observable where $H = \sum_i a_i P_k$, where $P_k \in \{I, X, Y, Z\}^{\otimes n}$. This method is naturally the most inaccurate.

4) Approximate Eigenvalue

If it is known our starting state ψ is close to an eigenstate (ψ_{λ_i}), where close is such that $\text{Tr} \sqrt{\sqrt{\psi} \psi_{\lambda_i} \sqrt{\psi}} \rightarrow 1$, we can treat the variance of the observable as negligible such that

$$\text{Var}(H) = \langle \psi | H^2 | \psi \rangle - \langle \psi | H | \psi \rangle^2 \approx E^2 - E^2 = 0. \quad (21)$$

Since $\Delta H = 0$, c will be a factor only of the noise sources.

B. CORRECTION OF VARIANCE

For some loose bound on the variance of the observable, we can correct it using the following method. Let's say that $\text{Var}(H) = \text{Var}_{\text{est}}(H) + E_h$, where we have chosen $\text{Var}_{\text{est}}(H)$. If we run the circuit to get a variance of H for a small number of shots we can then use that variance to correct our estimate of the variance of the observable. Naturally, the more shots we take, the more accurate our estimate of the variance of the observable will be but since everything is in log scale, we can afford to have approximate values.

Variance at a given number of shots is an inherently noisy value, which we can quantify as [21]

$$\text{Var}(\text{Var}(H)) = \frac{1}{n} \left(\mu_4 - \frac{n-3}{n-1} \sigma^4 \right). \quad (22)$$

In the interest of minimizing the error due to variance of variance, one may choose to apply Algorithm 1 to get a value of c_{real} for a slightly more resilient value of variance contained in it and then back substitute as,

$$\Delta H = \langle H \rangle 2^{2c_{\text{real}}} - \sum_i \text{Var}(X_i), \quad (23)$$

obtained by rearranging from (15).

Before getting into specific sources of noise it is also worth noting that the following methods assume no error correction has been applied, such as if T_1 noise has been corrected for, one may have to calculate a new effective T_1 value and apply it to the method or disregard it entirely if the error correction is approximately accurate.

C. SUPERCONDUCTING HARDWARE SPECIFIC

1) T_1, T_2 Effects

For both T_1, T_2 noise we can use their exponential decay models to estimate the variance of the noise, following our above assumption that it is independent of the state. So for some normalised time $\tau = t/T_i, T_i \in \{T_1, T_2\}$ we can write a stretched exponential decay as $\gamma_i = 1 - e^{-\tau^k}$, where k is some stretching factor, then the p^{th} moments of the distribution are given by,

$$\int_0^\tau \tau^p e^{-\tau^k} d\tau = \frac{1}{k} \gamma \left(\frac{p+1}{k}, \tau^k \right),$$

where γ is the lower incomplete Γ -function at circuit depth t . For $k = 1$ models of T_1, T_2 we can write the first and second moments as:

$$E_\tau(X) = 1 - (\tau + 1)e^{-\tau}, \quad (24)$$

$$E_\tau(X^2) = -\tau^2 e^{-\tau} + 2E_\tau(X). \quad (25)$$

It is worth noting that we have assumed all applied damping is of first order (Appendix VII-A), and that the damping is independent of the state of the qubit. For n qubits we can take the median T_1, T_2 values and apply them to all qubits as $(n \cdot \text{Var}_{T_i})$. For more conservative estimates one may choose to take the lowest T_1, T_2 values instead of the median and apply them to all qubits. One may even extend the model to a non-Markovian model of decay as shown in Appendix VII-C.

2) Gate Error

Any state ρ_i can be written in its eigenbasis as $\sum_{\lambda_i} a_i |\psi_{\lambda_i}\rangle$. We realize now that this state belongs to the space \mathcal{CP}^n (a $2n$ -manifold) via \mathcal{C}^{n+1} for any non-trivial state. In this space, we can now treat each gate as a transformation from one point to another where a gate error is some displacement measure $\xi^{(i)}, i \in [1, n]$ in each direction such that the state is transformed from its initial value ρ to $G\rho G^\dagger$, but is offset by some error Ξ_g . We will model this error as a random walk in the space \mathcal{CP}^n . Having assumed that gate errors are independent of the state of the qubit, and small, we can define an infidelity \mathcal{F}' as a function of the correct gate G and a noisy gate G' . Then for a state ρ , we can write the infidelity as,

$$\mathcal{F}'(G\rho G^\dagger, G'\rho G'^\dagger) = \|\Xi_g\|, \quad (26)$$

for a set of random variables such that

$$\Xi_{g,i} = (\xi_i^{(0)}, \xi_i^{(1)}, \dots, \xi_i^{(n)}) : \xi_i^{(j)} \sim W_i, \quad (27)$$

over n dimensions if W_i is the Wiener process in the j th dimension at some time t_i .¹ From the central limit theorem and Donsker's theorem [22], [23], we know such a random walk independently in each dimension is normally distributed. We write the variance of the gate noise as,

$$\sigma^2 = \frac{t}{\delta t} \epsilon^2. \quad (28)$$

Since we use a normalized depth D , we can directly write $D = \frac{t}{\delta t}$, and use Error Per Layered Gate (EPLG) as a two-qubit error estimate [24]. Then, a single qubit gate error is $\epsilon = \text{EPLG}/2$ and $\sigma^2 = D \cdot \text{EPLG}^2/4$. Therefore, the sum of variance in each dimension is now,

$$\sum_i \text{Var}(\xi^{(k)}) = n \cdot \frac{D \cdot \text{EPLG}^2}{4}. \quad (29)$$

For a large number of qubits, we can see we will clearly overestimate the gate noise, since the circuit may not be densely connected for n -qubits up to depth D . Due to a small number of qubits, we have chosen to ignore this effect here. One may choose to create a 'density' of gates, as a correction factor, should it be required.

¹We assume W_i is equal across all dimensions at some fixed time-step t_i .

3) Readout Error

Consider k independent bits X_i where:

- $X_i = 1$ transitions to 0 with probability p and stays 1 with probability $1 - p$.
- $X_i = 0$ transitions to 1 with probability q and stays 0 with probability $1 - q$.

The variance of each bit X_i is:

$$\text{Var}(X_i) = (1 - p + q)(p - q) \cdot 2^i. \quad (30)$$

We can see that for values of $p \approx q$ (as we saw before in $p_{0 \rightarrow 1}, p_{1 \rightarrow 0}$) the variance is 0 as long as 2^i is interpreted to remain 'small' in the result. If the numbers are taken bit-by-bit and joined in an integer (Ex. $101010_2 = 42_{10}$) we can see how the variance of the string grows will scale exponentially irrespective of p, q . However, if they are taken as a fraction such as in the phase estimation algorithm (Ex. $0.01101011_2 \approx 0.42_{10}$) where we treat each bit as a fraction of increasing precision, the variance will remain insignificant.

V. APPLICATION

We can now apply two separate tests to our method. First, we will check if the method is transferable across generations of IBM hardware. Then we will see if we can isolate the extra Δc due to just noise sources.

A. H_2 VQE

We construct a standard H_2 VQE with a 4-qubit Hartree Fock circuit in the STO-3G basis [25]. We have shown the Hamiltonian and the excitation-preserving circuit in Appendix VII-B for reference. In our case, we will use

$$\text{Var}(H) = \frac{(\lambda_{\max} - \lambda_{\min})^2}{4}, \quad (31)$$

which we can calculate in Python for the sake of demonstration. In practice, however, it is known that since we are using an initial Hartree Fock state the variance is already close to 0.

As assumed before, we treat T_1, T_2 as independent of each other and the circuit run. We can also assume approximate $\langle H \rangle = 1.84$ from known experimental results. We write the variance of the Hamiltonian with our first guess of $\text{Var}(H)$ as,

$$\text{Var}(H_2) = \text{Var}(H) + (4 \cdot \text{Var}(T_1) + 4 \cdot \text{Var}(T_2)). \quad (32)$$

to get the expected c values. Table 4 gives values of $c_{\text{pred}}, c_{\text{real}}, \Delta_\epsilon c$ for the H_2 VQE circuit on IBM Torino on 5 separate bunches of qubits. Each is chosen for similar T_1, T_2 values. We can see that mean $\Delta_\epsilon c = 1.68$ is very high since we overestimated variance. We can back substitute into (23) any of the c_{real} values (or the mean of them) to get the corrected variance of the Hamiltonian which in our case is $\frac{(\lambda_{\max} - \lambda_{\min})^2}{4} - 0.91$ where 0.91 was obtained from taking the mean of the variances we used to calculate the c_{real} values.

For the sake of robustness, we can demonstrate the experiment re-done on a different machine, IBM Osaka. We can see the results for the H_2 VQE circuit on IBM Osaka

TABLE 4: Results for H_2 VQE on IBM Torino.

Expt No.	T1	T2	c_{pred}	c_{real}	$\Delta_{\epsilon}c$
1	105	66	-0.851	-2.820	1.969
2	112	108	-0.851	-2.540	1.689
3	60	72	-0.851	-2.970	2.119
4	150	160	-0.836	-1.690	0.854
5	127	152	-0.851	-2.460	1.609

on 4 separate bunches of qubits. Each is chosen for similar T_1, T_2 values. The results are given in Table 5. We can see

TABLE 5: Results for H_2 VQE on IBM Osaka.

Expt No.	T1	T2	c_{pred}	c_{real}	$\Delta_{\epsilon}c$
1	140	58	-2.407	-3.030	0.623
2	208	84	-2.124	-1.590	0.534
3	268	99	-0.722	-0.610	0.112
4	222	66	-2.408	-2.070	0.338

that mean $\Delta_{\epsilon}c = 0.39$ is now close to 0 post-correction. As an example of application, we take the first row and calculate variances from our chosen parameters. We have the equation $y = -0.5x - 2.407$ (from $\log(\text{RSD}) = -\frac{1}{2} \log n + c$). Then, let's say at 2^8 shots $\log(\frac{\sigma}{\mu}) = -6.47$. Therefore, from $\mu = 1.84$, we have a $\sigma \approx 0.021$. From the data, we obtained $\sigma = 0.013$ for 2^8 shots, which we can see is reasonably close to the expected value and the difference can be explained by the $\Delta_{\epsilon}c$ we obtained.

Additionally, we can see if we treat the error as $\Delta_{\epsilon}c = \pm 1$ then the values of sigma we obtain would be within

$$\sigma_{\text{true}}/2 \leq \sigma \leq 2\sigma_{\text{true}}, \quad (33)$$

which in absolute values will get smaller and smaller, for smaller values of sigma, so for more shots even the window in the uncertainty of our uncertainty will get smaller.

It is worth noting above that the variance being referred to here is the variance of the circuit and the system, not the variance of the Hartree Fock model. For some minima $m \pm \sigma$ as predicted by this method, it is possible there exists a lower minima $m' \leq m - \sigma$ such that a different circuit may be able to find it in the absence of a proof of optimality of the circuit.

B. NOISE ISOLATION

With the above example, we should also be able to isolate the Δc due to just noise sources. To attempt to scale the method, we will now run it on the Li_2 VQE, which is 20 qubits and the approximate Hamiltonian is 1600 terms.

The way we will check if we can isolate the noise is by running the Li_2 Hartree Fock baseline circuit on Torino to get a reference c , then we can add an excitation preserving map to the circuit with very small rotations. We know that under small perturbed rotations the baseline results of the system Hamiltonian should be the same as the baseline circuit plus only the noise. We then subtract the c values of the baseline circuit from the c values of the perturbed circuit to get the Δc due to just noise.

For the sake of demonstration, in the previous section, we took median T_1, T_2 values and applied them to all qubits, here we will take the lowest T_1, T_2 values instead of the median and apply them to all qubits. We calculated the Δc values for the Li_2 VQE circuit on IBM Torino and got the following results: We can now again use the obtained variance from

TABLE 6: Results for plain Li_2 Hartree Fock on IBM Torino.

c_{pred}	c_{real}	$\Delta_{\epsilon}c$
-0.101	-4.630	4.529

this run to use as ΔH for our next run and get more accurate values for c . We will now calculate two rounds of c values for the Li_2 with one and two repetitions of excitation excitation-preserving map. As a side note, we can see anomalously the

TABLE 7: Results for Li_2 VQE with Excitation Preserving Map on IBM Torino.

Repetitions	c_{pred}	c_{real}	$\Delta_{\epsilon}c$
1	-3.030	-2.871	0.159
2	-3.180	-2.760	0.420

results for more repetitions are more accurate than for fewer repetitions, however, we suspect this is a random fluctuation. Our model clearly shows a predicted increase in the variance for two repetitions.

Extending this to actual predictions, if we take the first row then for our configuration of T_1, T_2, EPLG . We have the equation $y = -0.5x - 2.871$, then let's say at 2^9 shots $\log(\frac{\sigma}{\mu}) = -7.37$ i.e. $\frac{\sigma}{\mu} = 0.006$. We assumed the approximate expectation to be $\mu = \langle H \rangle = 16.3$ and therefore $\sigma = 0.098$. Therefore we can be sure that for 2^9 shots we should have approximately $\sigma \approx 0.098$, (real value was found to be 0.088). For a conservative guarantee we can round up to the next intercept and select $c = -2$, variance at 2^9 shots should be $\sigma < 0.19$.

The value found from the closed-form expression derived in Appendix VII-D was 0.068. Both these values are consistent with what we expect since the closed-form expression accounts for predefined known errors and is expected to underestimate variance for larger and larger circuits. Whereas the measure and estimate method uses real system data and therefore will be more accurate for larger values of shots even for large circuits.

VI. CONCLUSION AND FUTURE WORK

For small circuits, even our worst results are accurate to within $\Delta_{\epsilon}c = 1$. As a conservative estimate, we can always round to the next power of 2 for the same variance in the interest of guarantees of bounds. For all characterization-style experiments, we can estimate the number of shots required to slightly higher precision allowing for better system calibrations of quantum computers. An added benefit of a statistical approach is that it can also be used to benchmark simulators against real hardware since for a given form of

noise $\Delta_\epsilon c$ between hardware and simulator should be lower for better simulators.

It is also worth noting that we have followed the approach of finding c since we intend to avoid the inherent variation in the measurement of variance itself. If one does not wish to avoid it, one may use $\sigma_{n_1}^2/n_1 = \sigma_{n_2}^2/n_2$ for two different numbers of shots n_1, n_2 to get variance at the desired number of shots n . The estimation of variance there can be done from the direct expression derived in Appendix VII-D, and applied as

$$\text{Var}(H_{\text{noisy}}) = \text{Var}(H) + \sum_i \text{Var}(X_i), \quad (34)$$

or for $\text{Var}(H) \approx 0$. The increase in variance due to ‘noise’ $\sum_i \text{Var}(X_i)$ is,

$$\frac{n}{2s} \left(2 - \frac{\tau_1^2}{e^{\tau_1}} - \frac{\tau_2^2}{e^{\tau_2}} - \frac{(\tau_1 + 1)^2}{e^{2\tau_1}} - \frac{(\tau_2 + 1)^2}{e^{2\tau_2}} + \frac{tg^2}{2} \right), \quad (35)$$

for n qubits over s shots for $\tau_1 = t/T_1, \tau_2 = t/T_2$ and g is the gate error such that the circuit was run for a time t .

We have accounted only for the first orders of noise and ignored correlated all sources of noise. We, therefore, expect our models to be more inaccurate as the number of qubits increases by orders of magnitudes. Future scope for this work could be to account for more types of noise including correlated errors and crosstalk noise and to find patterns in higher-order noise terms.

VII. APPENDIX

A. FIRST ORDER APPROXIMATION

For E_k with $k \in \mathbb{Z}_2^n$ we can write,

- E_0 : occurs with probability $\mathcal{O}(1)$ order.
- E_1 : occurs with $\mathcal{O}(\gamma)$ order noise, such that the leading order term is γ or equivalently has a probability of $\mathcal{O}(\gamma)$.
- E_k : has $\mathcal{O}(\gamma^k)$ as higher order terms which we can ignore, such that if γ is small then probabilities of order $\mathcal{O}(\gamma^k)$ are negligible. [26]

This simplifies, for a given noise identical for n qubits, to reduce down to $n\mathcal{O}(\gamma)$ noise terms and Identity. Therefore for, p sources of noise, we need only $pn + 1$ terms to estimate the variance of the observable.

B. HYDROGEN VQE

The approximate Hamiltonian for H_2 in STO-3G basis is [27]

$$\begin{aligned} H = & 0.045YYYY + 0.045XXYY + 0.045YYXX \\ & + 0.045XXXX + 0.120IIZZ + 0.120ZZII \\ & + 0.166ZIIZ + 0.166IZZI + 0.168IZIZ \\ & + 0.170IIIZ + 0.170IZII + 0.17ZIZI \\ & - 0.219ZIII - 0.219IIZI - 0.815IIII. \end{aligned} \quad (36)$$

The circuit generated for the same is as shown in Fig. 12.

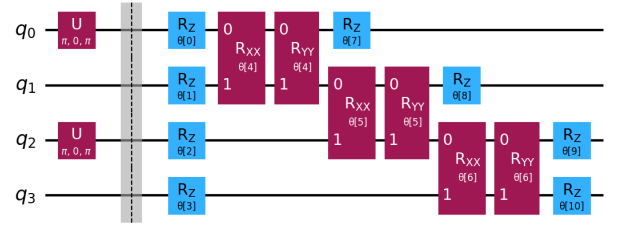


FIGURE 12: H_2 Hartree Fock initial circuit, followed by a hardware efficient excitation-preserving ansatz.

C. NON-MARKOVIAN DECAY

We treat our system as a two-level, open quantum system following the damped Jaynes-Cummings model. Then, the damping factor becomes a function of time as opposed to a constant, which we model as $\gamma(t) = 1 - |G(t)|^2$ where [28]:

$$G(t) = e^{-\frac{\lambda t}{2}} \left(\frac{\lambda}{d} \sinh \left[\frac{dt}{2} \right] + \cosh \left[\frac{dt}{2} \right] \right), \quad (37)$$

where $d = \sqrt{\lambda^2 - 2\gamma_0\lambda}$, γ_0 is the coupling strength of the system to the environment and λ is spectral band width. As before we can model its p^{th} moment as,

$$\int_0^{t_0} t^p |G(t)|^2 dt = \int_0^{t_0} t^p \left[e^{-\frac{\lambda t}{2}} \left(\frac{\lambda}{d} \sinh \frac{dt}{2} + \cosh \frac{dt}{2} \right) \right]^2 dt. \quad (38)$$

We can now substitute in the exponential forms of the hyperbolic functions and regroup to get,

$$\frac{1}{2} \int_0^{t_0} t^p \left[\left(\frac{\lambda}{d} + 1 \right) e^{-\frac{\lambda t}{2} + \frac{dt}{2}} - \left(\frac{\lambda}{d} - 1 \right) e^{-\frac{\lambda t}{2} - \frac{dt}{2}} \right]^2 dt. \quad (39)$$

We make a temporarily substitution $k = \frac{\lambda+d}{2}$ and $k' = \frac{\lambda-d}{2}$, and re-arrange

$$\begin{aligned} \frac{1}{d} \int_0^{t_0} t^p \left[k e^{-k't} - k' e^{-kt} \right]^2 dt &= \frac{k^2}{d} \int_0^{t_0} t^p e^{-2k't} dt \\ &+ \frac{k'^2}{d} \int_0^{t_0} t^p e^{-2kt} dt - \frac{2kk'}{d} \int_0^{t_0} t^p e^{-(k'+k)t} dt. \end{aligned} \quad (41)$$

We can then apply,

$$\int_0^{t_0} x^{t-1} e^{-cx} dx = \frac{1}{c^t} \int_0^{t_0} s^{t-1} e^{-s} ds = \frac{\gamma(t, t_0)}{c^t}, \quad (42)$$

to each term in the incomplete gamma function form to get

$$\begin{aligned} & \frac{k^2}{d} \frac{\gamma(p+1, t_0)}{(2k')^{p+1}} + \frac{k'^2}{d} \frac{\gamma(p+1, t_0)}{(2k)^{p+1}} - \frac{2kk'}{d} \frac{\gamma(p+1, t_0)}{(k'+k)^{p+1}} \\ &= \frac{\gamma(p+1, t_0)}{d} \left[\frac{k^2}{(2k')^{p+1}} + \frac{k'^2}{(2k)^{p+1}} - \frac{2kk'}{(k'+k)^{p+1}} \right]. \end{aligned} \quad (43)$$

Therefore for $p = 1$ we get the first moment as,

$$(1 - (t_0 + 1)e^{-t_0}) \left[\frac{k^2}{(2k')^2} + \frac{k'^2}{(2k)^2} - \frac{2kk'}{(k' + k)^2} \right] \\ = (1 - (t_0 + 1)e^{-t_0}) \left(\frac{-\Gamma_0}{\lambda} + \frac{1}{2} - \frac{2\lambda}{\Gamma_0} + \frac{\lambda^2}{\Gamma_0^2} \right). \quad (44)$$

And similarly, for $p = 2$ we get,

$$(-t_0^2 e^{-t_0} + 2(1 - (t_0 + 1)e^{-t_0})) \left(-\frac{\Gamma_0}{\lambda^2} + \frac{5}{4\Gamma_0} - \frac{5\lambda}{2\Gamma_0^2} + \frac{\lambda^2}{\Gamma_0^3} \right). \quad (45)$$

These resemble the results obtained for the standard case with the change of a constant factor.

D. DIRECT EXPRESSION

We can calculate the expression for the variance of ‘noise’ directly as:

$$\text{Var}(N) = \sum_i \text{Var}(X_i) = \text{Var}(T_1) + \text{Var}(T_2) + \text{Var}(G), \quad (46)$$

for T_1, T_2 and gate error G . We substitute the expression for variance of T_i via $E_\tau(X^2) - E_\tau(X)^2$ (from Section IV-C1) and for gate error as we modeled in Section IV-C2. So, the simplified variance for T_i till time τ would be

$$E_\tau(X^2) - E_\tau(X)^2 = 1 - \tau^2 e^{-\tau} - (\tau + 1)^2 e^{-2\tau}. \quad (47)$$

We substitute T_1, T_2 values and the gate error variance into the expression for variance per qubit as $\text{Var}(N) = \text{Var}(T_1) + \text{Var}(T_2) + \text{Var}(G)$, where

$$\text{Var}(N) = \frac{1}{2} - \frac{\tau_1^2}{2e^{\tau_1}} - \frac{(\tau_1 + 1)^2}{2e^{2\tau_1}} \\ + \frac{1}{2} - \frac{\tau_2^2}{2e^{\tau_2}} - \frac{(\tau_2 + 1)^2}{2e^{2\tau_2}} \\ + \frac{D \cdot \text{EPLG}^2}{4}. \quad (48)$$

For sake of simplicity, without change of notation assume we have written $\tau = t/T_i$ in units of δt , where our circuit ran for $t \cdot \delta t$ time out of $T_i \cdot \delta t$ time. Additionally, since we have already taken D , circuit depth in units of δt , we can write $D = t$, then with g as short for EPLG giving us finally for s shots, the sample variance for n qubits as:

$$\text{Var}(N) = \frac{n}{2s} \left(2 - \frac{\tau_1^2}{e^{\tau_1}} - \frac{\tau_2^2}{e^{\tau_2}} \right. \\ \left. - \frac{(\tau_1 + 1)^2}{e^{2\tau_1}} - \frac{(\tau_2 + 1)^2}{e^{2\tau_2}} + \frac{tg^2}{2} \right). \quad (49)$$

As before we maintain our core assumptions:

- Errors are independent of each other and the run circuit
- Circuits are well connected such that they cannot be easily cut into smaller circuits.

This variance of noise can be then used as is for single-shot experiments or added to the base variance of Hamiltonian $\text{Var}(H)$ for expectation value type experiments.

TABLE 8: Results for T_1 VQE on IBM Torino.

Qubit	Real c	Wait	T_1	Pred c	Error
69	2.021	10h	209	0.00285	-2.0182
65	2.298	10h	227	0.0097	-2.2883
59	2.176	10h	107	0.0233	-2.1527
29	-0.129	1000x	144	0.25385	+0.3829
120	0.024	100x	111	0.03795	+0.0139
103	-0.235	10x	244	0.0228	+0.2578
86	0.319	1000id	164	0.3419	+0.0229
82	0.647	1000id	134	0.3255	-0.3215
44	-0.288	100id	248	0.01855	+0.3066
31	0.319	10id	179	-0.0097	-0.3287
27	-0.041	10id	150	0.0585	+0.0995
23	-0.033	10id	159	0.01815	+0.0512
4	0.161	10id	153	0.03975	-0.1212
62	2.869	10h	128	0.0304	-2.8386
57	2.221	10h	177	-0.00035	-2.2214
33	0.030	1000x	45	1.0786	+1.0486
26	0.139	1000x	219	0.11775	-0.0213
22	0.127	1000x	70	0.5631	+0.4361
20	0.307	1000x	172	0.25515	-0.0519
128	-0.227	100x	184	0.0079	+0.2349
123	-0.036	100x	91	0.4004	+0.4364
106	0.281	10x	135	0.03855	-0.2425
100	0.014	10x	26	0.19965	+0.1856
98	-0.031	10x	70	0.04015	+0.0711
95	-0.065	10x	281	-0.00385	+0.0612
90	0.261	1000id	222	0.1636	-0.0974
79	2.299	1000id	56	0.7078	-1.5912
76	0.111	1000id	203	0.1912	+0.0802
52	-0.178	100id	190	0.0059	+0.1839
47	0.075	100id	192	0.0434	-0.0316
41	0.031	100id	39	0.1724	+0.1414
38	0.153	100id	208	0.0392	-0.1138
0	0.112	10id	49	0.0278	-0.0842
130	0.329	100x	249	0.0234	-0.3056
129	0.283	100x	225	0.0305	-0.2525
14	-0.004	10id	205	0.0131	+0.0171

E. DATA TABLES REFERENCES

- [1] Peter W. Shor. Polynomial-time algorithms for prime factorization and discrete logarithms on a quantum computer. *SIAM Journal on Computing*, 26(5):1484–1509, October 1997.
- [2] Juan Miguel Arrazola, Olivia Di Matteo, Nicolás Quesada, Soran Jahangiri, Alain Delgado, and Nathan Killoran. Universal quantum circuits for quantum chemistry. *Quantum*, 6:742, June 2022.
- [3] John Preskill. Quantum computing in the nisq era and beyond. *Quantum*, 2:79, August 2018.
- [4] Alberto Peruzzo, Jarrod McClean, et al. A variational eigenvalue solver on a photonic quantum processor. *Nature Communications*, 5(1), July 2014.
- [5] Ryan Sweke, Frederik Wilde, et al. Stochastic gradient descent for hybrid quantum-classical optimization. *Quantum*, 4:314, August 2020.
- [6] Jonathan J. Burnett, Andreas Bengtsson, Marco Scigliuzzo, David Niepe, Marina Kudra, Per Delsing, and Jonas Bylander. Decoherence benchmarking of superconducting qubits. *npj Quantum Information*, 5(1), 2019.
- [7] Malcolm S. Carroll, James R. Wootton, and Andrew W. Cross. Subsystem surface and compass code sensitivities to non-identical infidelity distributions on heavy-hex lattice. *arXiv:2402.08203*, 2 2024.
- [8] Kevin J Sung, Jiahao Yao, et al. Using models to improve optimizers for variational quantum algorithms. *Quantum Science and Technology*, 5(4):044008, September 2020.
- [9] Eric G. Brown, Oktay Goktas, et al. Quantum amplitude estimation in the presence of noise. *arXiv:2006.14145*, 2020.
- [10] Samantha V. Barron, Daniel J. Egger, Elijah Pelofske, Andreas Bärttschi, Stephan Eidenbenz, Matthias Lehmkuehler, and Stefan Woerner. Provable bounds for noise-free expectation values computed from noisy samples. *Nature Computational Science*, Nov 2024.

TABLE 9: Results for T_2 VQE on IBM Torino.

Qubit	Real c	Wait	T_2	Pred c	Error
132	1.705	1000x	248	1.69195	0
122	1.471	1000x	198	1.72975	+0.2587
119	1.128	1000x	189	1.5337	+0.4057
129	1.478	1000x	108	1.3183	-0.1597
106	2.332	100x	102	2.68935	+0.3574
103	2.439	100x	74	2.33025	-0.1088
100	1.932	100x	102	1.8333	-0.0987
98	2.437	100x	42	2.1786	-0.2584
95	1.893	100x	251	2.0673	+0.1743
90	2.017	10x	243	2.40365	+0.3866
86	1.697	10x	110	2.2068	+0.5098
82	2.117	10x	49	2.3032	+0.1862
79	3.369	10x	27	3.1164	-0.2526
76	2.250	10x	249	2.8191	+0.5691
69	0.048	10h	63	2.33465	+2.2866
65	-0.083	10h	183	3.4123	+3.4953
62	-0.076	10h	130	3.19865	+3.2747
59	0.196	10h	157	2.9494	+2.7534
57	0.134	10h	126	2.78015	+2.6462
52	2.772	1000id	229	1.69315	-1.0788
47	1.607	1000id	66	1.01545	-0.5916
44	1.151	1000id	209	1.6686	+0.5176
41	0.042	1000id	47	0.83915	+0.7971
38	1.807	1000id	87	0.94685	-0.8602
33	1.283	100id	189	1.2426	-0.0404
29	3.053	100id	132	2.3249	-0.7281
26	2.634	100id	175	2.45065	-0.1833
23	3.002	100id	188	2.36855	-0.6334
20	2.047	100id	95	2.7289	+0.6819
14	2.545	10id	152	2.4342	-0.1108
9	3.339	10id	184	3.4468	+0.1078
7	1.875	10id	138	2.89255	+1.0176
4	2.484	10id	176	3.1593	+0.6753
0	1.752	10id	96	1.99225	+0.2403

duction to the Theory of Statistics. McGraw-Hill, New York, 3rd edition, 1974.

- [22] Monroe D. Donsker. An invariance principle for certain probability limit theorems. In Four Papers on Probability, volume 6 of Memoirs of the American Mathematical Society, pages 50–61. American Mathematical Society, Providence, Rhode Island, 1951.
- [23] Paul Erdős and Mark Kac. On certain limit theorems of the theory of probability. Bulletin of the American Mathematical Society, 52:292–302, 1946.
- [24] David C. McKay, Ian Hincks, Emily J. Pritchett, Malcolm Carroll, Luke C. G. Govia, and Seth T. Merkel. Benchmarking quantum processor performance at scale. arXiv:2311.05933, 2023.
- [25] Qiming Sun, Xing Zhang, Samragni Banerjee, and Bao et al. Recent developments in the pyscf program package. The Journal of Chemical Physics, 153(2), July 2020.
- [26] Sourav Dutta, Debjyoti Biswas, and Prabha Mandayam. Noise-adapted qudit codes for amplitude-damping noise. arXiv:2406.02444, 2024.
- [27] Sam McArdle, Suguru Endo, Alán Aspuru-Guzik, Simon C. Benjamin, and Xiao Yuan. Quantum computational chemistry. Rev. Mod. Phys., 92:015003, Mar 2020.
- [28] Heinz-Peter Breuer, Elsi-Mari Laine, Jyrki Piilo, and Bassano Vacchini. Colloquium: Non-markovian dynamics in open quantum systems. Rev. Mod. Phys., 88:021002, Apr 2016.

...

[11] Acharya R, Abanin D. A, Aghababaie-Beni L, Aleiner I, Andersen T, Google Quantum AI, and Collaborators. Quantum error correction below the surface code threshold. Nature, Dec 2024.

[12] Michael R Geller and Mingyu Sun. Toward efficient correction of multiqubit measurement errors: pair correlation method. Quantum Science and Technology, 6(2):025009, February 2021.

[13] P. Krantz, M. Kjaergaard, F. Yan, T. P. Orlando, S. Gustavsson, and W. D. Oliver. A quantum engineer’s guide to superconducting qubits. Applied Physics Reviews, 6(2), June 2019.

[14] Fangzhao Alex An, Anthony Ransford, Andrew Schaffer, Lucas R. Sletten, John Gaebler, James Hostetter, and Grahame Vittorini. High fidelity state preparation and measurement of ion hyperfine qubits with $i > 1/2$. Physical Review Letters, 129(13), September 2022.

[15] Thomas Strohm, Karen Wintersperger, Florian Dommert, Daniel Basilewitsch, Georg Reuber, and Andrey Hoursanov et al. Ion-based quantum computing hardware: Performance and end-user perspective. arXiv:2405.11450, 2024.

[16] Sergey Bravyi, Matthias Englbrecht, Robert König, and Nolan Peard. Correcting coherent errors with surface codes. npj Quantum Information, 4(1), October 2018.

[17] Daniel Greenbaum and Zachary Dutton. Modeling coherent errors in quantum error correction. Quantum Science and Technology, 3(1):015007, December 2017.

[18] Giovanni Di Bartolomeo, Michele Vischi, Francesco Cesa, Roman Wixinger, Michele Grossi, Sandro Donadi, and Angelo Bassi. Noisy gates for simulating quantum computers. Phys. Rev. Res., 5:043210, Dec 2023.

[19] Conrad Strydom and Mark Tame. Measurement-based interleaved randomised benchmarking using ibm processors. Physica Scripta, 98(2), January 2023.

[20] Rajendra Bhatia and Chandler Davis. A better bound on the variance. The American Mathematical Monthly, 107(4):353–357, 2000.

[21] Alexander M. Mood, Franklin A. Graybill, and Duane C. Boes. Intro-